AIAA JOURNAL
Vol. 53, No. 10, October 2015

# Micromechanics of Composites Using a Two-Parameter Model and Response Surface Predictions

Ashesh Sharma* and Bhavani V. Sankar†
*University of Florida, Gainesville, Florida 32611*

DOI: 10.2514/1.J053804

**A novel method involving the use of micromechanical analysis to predict elastic constants of a unidirectional fiber-reinforced composite is proposed. The method revolves around a model called the two-parameter model. The two parameters are obtained by performing one micromechanical analysis of the composite unit cell along one of its transverse directions. The method involves construction of response surfaces that act as surrogate models, for the prediction of the two parameters, corresponding to any fiber-reinforced composite design that uses a transversely isotropic fiber and an isotropic matrix. Using the two parameters, four of the five elastic constants can be computed. The fifth elastic constant, longitudinal shear modulus, is predicted using a separate response surface. The results indicate that the two-parameter model in conjunction with the response surface makes accurate prediction of composite elastic constants.**



## Nomenclature

| | | |
|---|---|---|
| $C$ | = | stiffness matrix of the composite |
| $C_f$, $C_m$ | = | stiffness matrix of fiber, matrix materials |
| $E_{f1}$ | = | longitudinal Young's modulus of fiber |
| $E_{f2}$, $E_{f3}$ | = | transverse Young's modulus of fiber in 2- or 3-direction |
| $E_m$ | = | Young's modulus of matrix |
| $E_1$ | = | longitudinal Young's modulus of composite |
| $E_2$, $E_3$ | = | transverse Young's modulus of composite in 2- or 3-direction |
| $G_{12}$ | = | shear modulus of composite in the longitudinal direction |
| $G_{f12}$ | = | longitudinal shear modulus of fiber |
| NEFL | = | number of fiber elements |
| $[T]$ | = | influence matrix relating average fiber strains to macrostrains in composite |
| $u_i$ | = | displacement along the $i$th direction |
| $\bar{u}_{1a}$, $\bar{u}_{1b}$ | = | average $u_1$ displacements of points on surfaces $a$, $b$ |
| $\bar{u}_{f1a}$, $\bar{u}_{f1b}$ | = | average $u_1$ displacements of fiber on surfaces $a$, $b$ |
| $V_f$ | = | fiber volume fraction |
| $V_f$, $V_m$ | = | volume of fiber, matrix phases |
| $V$ | = | volume of composite |
| $x_i$ | = | Cartesian coordinates |
| $[\Delta]$ | = | difference between stiffness matrices of fiber and matrix material |
| $\varepsilon$ | = | strain |
| $\bar{\varepsilon}_f$ | = | average fiber strain |
| $\varepsilon^M$ | = | macrostrain (average strain) in the composite |
| $\varepsilon^M_{ii}$ | = | macrostrain in the composite in the $i$th direction |
| $\varepsilon^{(e)}$ | = | strains at the centroid of element $e$ |
| $\nu_{f12}$ | = | major Poisson's ratio of fiber |
| $\nu_{f23}$ | = | transverse Poisson's ratio of fiber |
| $\nu_m$ | = | Poisson's ratio of matrix |
| $\nu_{12}$ | = | major Poisson's ratio of composite |
| $\nu_{23}$ | = | transverse Poisson's ratio of composite |
| $\sigma^M$ | = | macrostress (average stress) in the composite |

Received 20 August 2014; revision received 19 December 2014; accepted for publication 28 February 2015; published online 24 April 2015. 

*Graduate Student; currently University of Colorado, Boulder.
†Ebaugh Professor, Department of Mechanical and Aerospace Engineering. Associate Fellow AIAA.

## I. Introduction

MICROMECHANICS has been a widely adopted approach for the prediction of effective properties of a composite material. For more than a century, researchers have developed various analytical methods such as rule of mixtures [1] and mean field methods (e.g., Eshelby [2]), leading to the derivation of semi-empirical formulas such as the Halpin–Tsai equations [3] for the calculation of effective properties. Finite-element-based micromechanics has been quite popular for unidirectional composites for predicting elastic constants (e.g., Sun and Chen [4]) and for predicting strength properties (e.g., Zhu et al. [5]). Jadhav and Sridharan [6] made use of finite-element-based micromechanics for the prediction of nonlinear response of laminated composites. Dang and Sankar [7] used the meshless local Petrov–Galerkin in micromechanical models for predicting the elastic constants of composites. Rakow and Waas [8] used micromechanics approach for random fiber composites. Chou and Ishikawa [9] and Bednarcyk and Arnold [10] made use of micromechanics to predict the elastic properties of woven fabric and woven polymer composites, respectively. Tabiei et al. [11] used micromechanics for analysis of plane-weave-fabric composites with nonlinear material behavior. Recently, Weigand and TerMaath [12] have used finite-element-based micromechanics for sensitivity analysis of composite properties.

Advanced fiber composites have been used in aerospace and other industries for more than 50 years. Advances in low-cost manufacturing techniques have made it possible to use fiber composites in many other applications (e.g., wind-turbine blade, sporting goods, boats, and other vehicles). In addition, textile composites such as woven and braided composites are widely used in the aforementioned applications. However, estimation of the properties of textile composites requires the properties of the unidirectional composites made of the fiber tow and the matrix. There is a need for efficient and accurate methods to estimate the properties of the composites from the fiber and matrix properties. Although finite-element-based micromechanics and testing can be afforded by big industries, small companies need simpler methods to estimate the mechanical properties of the composites at design stage. Furthermore, accurate closed-form expressions for properties are useful in the design optimization stage.

There are several methods available in the literature for estimating the properties of unidirectional composites. For example, the rule of mixtures is found to yield accurate results for the longitudinal modulus $E_1$ and the major Poisson's ratio $\nu_{12}$. For transverse properties such as $E_2$ and longitudinal shear modulus $G_{12}$, the Halpin–Tsai equations are popular. However, Halpin–Tsai types of equations are not available for hexagonal unit cells [13,14].

In the present study, we make use of polynomial response surfaces to derive empirical equations for various elastic constants in terms of nondimensional fiber and matrix properties and fiber volume fraction. Although one can construct response surfaces for each of the elastic constants, we have simplified the approach by identifying two parameters in the micromechanics equations that describe four of the five elastic constants of a transversely isotropic composite. This model is referred to as the two-parameter model (TPM) in the paper, and thus the response surfaces are constructed only for the two parameters. The accuracy of the model is verified by comparing the empirical results with that of finite-element analyses for various composite material systems. It is found that the current empirical relations are very accurate when compared to results from finite-element analysis (FEA). The elastic constants predicted using the two-parameter model are $E_1, E_2, \nu_{12}$, and $\nu_{23}$, where fiber is aligned in the 1-direction. It is noted that $G_{23}$ may be computed using $E_2$ and $\nu_{23}$, and hence is not treated as an independent elastic constant [15]. Independent of the TPM, a separate response surface is constructed for the prediction of the longitudinal shear modulus $G_{12}$, so that surrogate models for all the independent elastic constants of a transversely isotropic composite will be available. All response surfaces were constructed using the surrogate toolbox developed by Viana [16].

The paper is structured as follows. Section II presents the derivation of the two-parameter model. In Sec. III, surrogate models for accurate prediction of elastic constants have been presented. Section IV discusses the accuracy of the proposed method. In Sec. V, a separate response surface for the prediction of the longitudinal shear modulus has been presented, and conclusions are given in Sec. VI. A brief explanation of various error measures used in the surrogate models are provided in the Appendix.

## II. Two-Parameter Model

### A. Derivation of the Two-Parameter Model

For the derivation of the two-parameter micromechanical model for a finite medium, fibers are assumed of circular cross section, packed in a square or hexagonal array. No sort of isotropy is associated with the fiber or the matrix.

We use $\sigma^M$ and $\varepsilon^M$ to refer to the macrostresses and macrostrains in the composite. Our goal is to determine the stiffness matrix $C$ of the composite that relates the macrostresses and strains as

$$\sigma^M = C\varepsilon^M \tag{1}$$

The macrostrains can be expressed as the volume average of the microstrains: strains averaged over the unit cell. Then, the previous constitutive equation can be written as

$$\sigma^M = C\varepsilon^M \quad = \frac{1}{V}\int_{V_f} C_f\varepsilon \,\mathrm{d}V + \frac{1}{V}\int_{V_m} C_m\varepsilon \,\mathrm{d}V \tag{2}$$

Here, $\varepsilon$ are the microstrains or simply strains in the fiber or the matrix phases; $V_f$ and $V_m$, respectively, are the volumes of the fiber and matrix phases ($V = V_f \cup V_m$); and $C_f$ and $C_m$ are the stiffness matrices of the fiber and matrix materials, respectively. In Eq. (2), the integration has been split into two parts: one over the fiber phase ($V_f$) and the other over the matrix phase ($V_m$). We modify the previous equation by adding and subtracting $C_m$ in the first integral and use some algebraic manipulation to obtain

$$\begin{aligned} C\varepsilon^M &= \frac{1}{V}\int_{V_f}[C_f - C_m + C_m]\varepsilon \,\mathrm{d}V + \frac{1}{V}\int_{V_m}[C_m\varepsilon]\,\mathrm{d}V \\ &= \frac{1}{V}\int_{V_f}[C_f - C_m]\varepsilon \,\mathrm{d}V + \left[\frac{1}{V}\int_{V_m}(C_m\varepsilon)\,\mathrm{d}V + \frac{1}{V}\int_{V_f}(C_m\varepsilon)\,\mathrm{d}V\right] \\ &= \frac{1}{V}\int_{V_f}[C_f - C_m]\varepsilon \,\mathrm{d}V + \frac{1}{V}\int_{V}[C_m\varepsilon]\,\mathrm{d}V \end{aligned} \tag{3}$$

We now multiply and divide the first term on the right-hand side of the previous equation with the fiber volume $V_f$, and note the second integral represents the average or macrostrains in the composite. Thus, we can derive

$$C\varepsilon^M = V_f[C_f - C_m]\int_{V_f}\frac{1}{V_f}(\varepsilon)\,\mathrm{d}V + C_m\varepsilon^M \tag{4}$$

$V_f$ is the fiber volume fraction of the composite. Now, the integral in Eq. (4) can be recognized as average fiber strain $\bar{\varepsilon}_f$, and we finally arrive at the relation

$$C\varepsilon^M = V_f[C_f - C_m]\bar{\varepsilon}_f + C_m\varepsilon^M \tag{5}$$

Because we are in the realm of linear elasticity, the average strains in the fiber will be linearly related to the macroscopic strains in the composite:

$$\{\bar{\varepsilon}_f\} = [T]\{\varepsilon^M\} \tag{6}$$

In the previous equation, $[T]$ is a constant square matrix, and it depends only on the material properties and the microstructure including fiber volume ratio. Then, Eq. (5) can be written as

$$C\varepsilon^M = V_f[C_f - C_m][T]\varepsilon^M + C_m\varepsilon^M \tag{7}$$

If the previous relation must be true for any arbitrary state of macrostrain $\varepsilon^M$, then the following identity must also hold true:

$$C = C_m + V_f[C_f - C_m][T] \tag{8}$$

That is, the only information we need to calculate the stiffness of the composite is the influence matrix $[T]$ for a given material and microstructure. Subsequently, Eq. (8) can be used to determine the composite elastic constants in terms of fiber and matrix properties as well as fiber volume fraction.

The preceding discussion is independent of the microstructure. In the following, we discuss the special form $[T]$ takes in the case of unidirectional fiber composites. For the purpose of illustration, we use a hexagonal unit cell, although the discussions are valid for other shapes such as square unit cell as long as the fiber occupies the entire length of the unit cell in the 1-direction. Referring to Fig. 1, the macrostrain along the 1-direction, $\varepsilon_{11}^M$, can be written as

$$\varepsilon_{11}^M = \frac{1}{V}\int_V \frac{\partial u_1}{\partial x_1}\,\mathrm{d}V \tag{9}$$

Making use of basic calculus and algebra (also shown in [15]), the previous strain can be expressed as

$$\varepsilon_{11}^M = \frac{1}{L_1}(\bar{u}_{1a} - \bar{u}_{1b}) \tag{10}$$

where $\bar{u}_{1a}$ and $\bar{u}_{1b}$ are the average $u_1$ displacements on surface $a(L_1, x_2, x_3)$ and surface $b(0, x_2, x_3)$ ; see Fig. 1. Using a similar procedure, the average strain $\bar{\varepsilon}_{f11}$, in the unidirectional fiber can be derived as

$$\bar{\varepsilon}_{f11} = \frac{1}{L_1}(\bar{u}_{f1a} - \bar{u}_{f1b}) \tag{11}$$

where the average is performed only over the two end faces of the fiber. However, periodic boundary conditions dictate that $(\bar{u}_{1a} - \bar{u}_{1b})$ is a constant, and it is equal to $(\bar{u}_{f1a} - \bar{u}_{f1b})$. Thus, one can show that

$$\varepsilon_{11}^M = \bar{\varepsilon}_{f11} \tag{12}$$

The $T$ matrix, by definition, is of the form

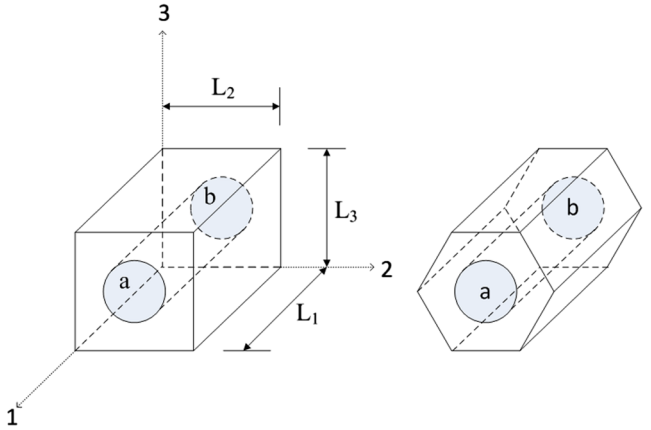


**Fig. 1 Unidirectional fiber surrounded by matrix comprising square and hexagonal unit cells. The end surfaces of the unit cell are denoted by "a" and "b".**

$$\begin{Bmatrix} \bar{\varepsilon}_{f11} \\ \bar{\varepsilon}_{f22} \\ \bar{\varepsilon}_{f33} \end{Bmatrix} = \begin{bmatrix} T_{11} & T_{12} & T_{13} \\ T_{21} & T_{22} & T_{23} \\ T_{31} & T_{32} & T_{33} \end{bmatrix} \begin{Bmatrix} \varepsilon_{11}^M \\ \varepsilon_{22}^M \\ \varepsilon_{33}^M \end{Bmatrix} \tag{13}$$

Then, it is obvious from Eq. (12) that $T_{11} = 1$ and $T_{12} = T_{13} = 0$. As will be shown later for square and hexagonal unit cells considered in this paper, $T_{22} = T_{33}$ and $T_{23} = T_{32}$ due to symmetry of the unit cell.

Now, let us consider Eq. (8). The stiffness matrices $[C]$ and $[C_f]$ are symmetric. Hence, the product $[C_f - C_m][T]$ must be symmetric. Denote the difference between the stiffness matrices of fiber and matrix as $[\Delta]$. Then,

$$\begin{aligned}
&[C_f - C_m][T] \\
&= \begin{bmatrix} \Delta_{11} & \Delta_{21} & \Delta_{21} \\ \Delta_{21} & \Delta_{22} & \Delta_{32} \\ \Delta_{21} & \Delta_{32} & \Delta_{22} \end{bmatrix} \begin{bmatrix} 1 & 0 & 0 \\ T_{21} & T_{22} & T_{32} \\ T_{31} & T_{32} & T_{22} \end{bmatrix} \\
&= \begin{bmatrix} \Delta_{11} + \Delta_{21}(T_{21} + T_{31}) & \Delta_{21}(T_{22} + T_{32}) & \Delta_{21}(T_{22} + T_{32}) \\ \Delta_{21} + \Delta_{22}T_{21} + \Delta_{22}T_{22} & \Delta_{22}T_{22} + \Delta_{32}T_{32} & \Delta_{32}T_{22} + \Delta_{22}T_{32} \\ \Delta_{21} + \Delta_{32}T_{21} + \Delta_{22}T_{31} & \Delta_{32}T_{22} + \Delta_{22}T_{32} & \Delta_{22}T_{22} + \Delta_{32}T_{32} \end{bmatrix}
\end{aligned} \tag{14}$$

The symmetry condition of the previous product leads to

$$\begin{aligned}
\Delta_{21} + \Delta_{22}T_{21} + \Delta_{32}T_{31} &= \Delta_{21}(T_{22} + T_{32}) \\
\Delta_{21} + \Delta_{32}T_{21} + \Delta_{22}T_{31} &= \Delta_{21}(T_{22} + T_{32})
\end{aligned} \tag{15}$$

The previous equations can be solved to express $T_{21}$ and $T_{31}$ in terms of $T_{22}$ and $T_{32}$:

$$T_{21} = T_{31} = \frac{\Delta_{12}(T_{22} + T_{32} - 1)}{\Delta_{22} + \Delta_{23}} \tag{16}$$

Thus, the two parameters $T_{22}$ and $T_{32}$. completely define $[T]$. The following subsection shows how both terms can be obtained by performing one micromechanical analysis.

The physical meaning of the previous two parameters will be useful in calculating them using the FEA. $T_{22}$ is the average fiber strain $\bar{\varepsilon}_{f22}$ when the representative volume element (RVE) is subjected to only unit macrostrain $\varepsilon_{22}^M$, (i.e., when $\varepsilon_{11}^M = \varepsilon_{33}^M = 0$, $\varepsilon_{22}^M = 1$). Similarly, $T_{32}$ is the average fiber strain $\bar{\varepsilon}_{f33}$ when the RVE is subjected to only unit macrostrain $\varepsilon_{22}^M$. That means by performing one micromechanical analysis of the RVE with $\varepsilon_{11}^M = \varepsilon_{33}^M = 0$, $\varepsilon_{22}^M = 1$, we can claulctae both the parameters $T_{32}$ and $T_{32}$.

### B. Calculating the T Matrix

We are only interested in composites with transversely isotropic or isotropic fibers with a hexagonal unit cell. For composites with hexagonal unit cell, a rectangular RVE has been used, which effectively encompasses two complete hexagonal unit cells (Fig. 2). Furthermore, we will consider only one quarter of the rectangle due to symmetry (Fig. 3), and thus the size of the model, hence the computational cost, is further reduced. We chose a rectangular RVE because of ease of applying multipoint constraints in the finite-element model.

The finite-element model corresponds to a hexagon with an edge length of one unit. This results in a rectangular RVE of edge length of 1.5 units along the 2-direction and 0.866 units along the 3-direction. A plane strain element with unit thickness is used for the micromechanical analysis, which was carried out using Abaqus, a commercial finite-element software. A total of 612 quadrilateral elements were used in one quarter of the rectangular unit-cell (Fig. 3). A convergence analysis using graphite/epoxy composite system was carried out to confirm the accuracy of the finite-element model [15]. Boundary conditions applied to the representative volume elements correspond to a unit strain analysis. That is, for a micromechanical analysis along either of the transverse directions, unit strain is applied along the respective direction. One may refer to [15] for applying periodic boundary conditions using multipoint constraints in FEA. Strains were computed at the centroid of each fiber element to calculate the average fiber strains $\bar{\varepsilon}_{f22}$ and $\bar{\varepsilon}_{f33}$.

For an initial testing of the model given by Eq. (8), finite-element-based unit strain analysis was performed using two designs with fiber volume fraction 0.6. The first design uses a transversely isotropic graphite fiber [17], and the other uses an isotropic E-glass fiber [18]. Because we are interested only in isotropic materials for the matrix, epoxy [18] was used for both examples.

We consider two cases, 1) $\varepsilon_{22}^M = 1$;, and 2) $\varepsilon_{33}^M = 1$;, to validate $T_{22} = T_{33}$ and $T_{22} = T_{32}$. The former will provide us with $T_{22}$ and

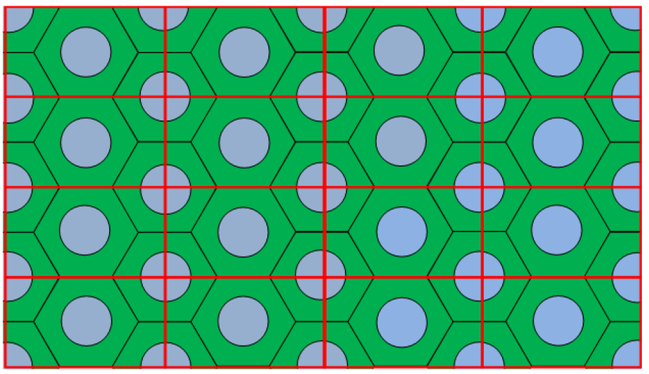

**Fig. 2 Representative volume elements for composites with hexagonal unit cells.**

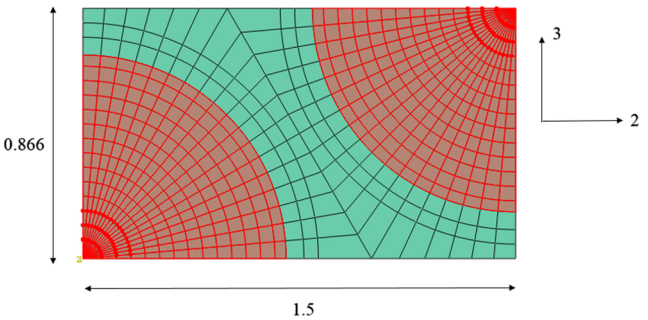


**Fig. 3 One-fourth representative volume element (RVE) for composites with hexagonal unit cells. The RVE contains a quadrant of two adjacent fibers.**

$T_{32}$. Similarly, case 2 will yield $T_{23}$ and $T_{33}$. Let us take the example of case 1, wherein unit strain is applied along the 2-direction. To compute the average strains $\bar{\varepsilon}_{f22}$ and $\bar{\varepsilon}_{f33}$ in the fiber, the elemental strains $\varepsilon_{22}$ and $\varepsilon_{33}$ were computed at the centroid of fiber elements, and the following calculations were used to determine the average fiber strains:

$$\bar{\varepsilon}_{fii} = \frac{\sum_1^{\text{NEFL}} \varepsilon_{ii}^{(e)} V^{(e)}}{\sum_1^{\text{NEFL}} V^{(e)}}, \qquad i = 2, 3 \tag{17}$$

where $V_{(e)}$ is the volume and $\varepsilon_{ii}^{(e)}$ is the strain in the $e$th element; NEFL is the total number of fiber elements and the sum is performed over the fiber elements. When $\varepsilon_{11}^M = \varepsilon_{33}^M = 0$, $T_{22} = \bar{\varepsilon}_{f22}/\varepsilon_{22}^M$; $T_{32} = \bar{\varepsilon}_{f33}/\varepsilon_{22}^M$.

Upon performing micromechanical analysis of the models for composites with hexagonal unit cells, it was observed that $T_{22} \cong T_{33}$ and $T_{32} = T_{23}$. The relevant results are given in Table 1. Based on the results in Table 1, it can be deduced that there is absolutely no requirement to perform micromechanical analyses along both the transverse axes, 2 and 3. Instead, only one analysis is sufficient to provide us with the values of $T_{22}$, $T_{32}$, $T_{33}$, and $T_{23}$.

## III. Developing Surrogate Models for $T_{22}$ and $T_{32}$

A response surface methodology portrays the relationship between several explanatory (independent) variables and one or more response (dependent) variables. The method was first introduced by Box and Wilson in 1951 [19]. It is important to acknowledge that this model is only an approximation but is widely used because such a model is easy to estimate and apply, even when little is known about the process. Basic terminologies and error measures involved in fitting an approximation to a set of data have been further discussed in detail in the Appendix.

For creating our design of experiments, a design space was generated using the Latin hypercube sampling (LHS) function provided in MATLAB. A big advantage of using LHS design space is that the design points are better distributed for each variable. A potential problem with the method is that, even though the design points are well spread out, there are still some voids left in between the data points. To overcome this problem, we perform multiple iterations of LHS design in an attempt to maximize the minimum distance between design points. This helps to populate the entire design space. A more comprehensive study on the topic of response surface methodology has been presented in [20,21]. It is important to note that the LHS function in MATLAB requires the design variables be in the range of zero to 1. Hence the actual design variables have to be scaled to keep 0–1 as the range.

As shown earlier, the knowledge of $T_{22}$ and $T_{32}$ is sufficient enough for the prediction of the stiffness matrix of the composite and, thus, the prediction of materials constants $E_1, E_2, \nu_{12}$, and $\nu_{23}$. Hence, it is sufficient to build response surfaces for the two parameters $T_{22}$ and $T_{32}$. The response surfaces have been constructed only for circular fibers in a hexagonal array. The independent variables for the response surface will be the fiber elastic constants $E_{f1}, E_{f2}, \nu_{f12}$, and $\nu_{f23}$; matrix elastic constants $E_m$, and $\nu_m$; and the fiber volume ratio $V_f$. Further, the number of design variables could be reduced by nondimensionalizing the variables, as shown in Eq. (18). The range of the material constants were chosen based on the data for various composites available in literature:

**Table 1 Results from unit strain analysis along the transverse directions**

| Composite | $T_{22}$ | $T_{33}$ | $T_{32}$ | $T_{23}$ |
|---|---|---|---|---|
| *Hexagonal unit cell* | | | | |
| Graphite/epoxy | 0.5406 | 0.5403 | 0.0326 | 0.0326 |
| Glass/epoxy | 0.2051 | 0.2049 | 0.0286 | 0.0286 |

$$20 < \frac{E_{f1}}{E_m} < 120; \qquad 1 < \frac{E_{f1}}{E_{f2}} < 35; \qquad 1 < \frac{G_{f12}}{G_m} < 30;$$
$$0.2 < \nu_{f12} < 0.35; \quad 0.35 < \nu_{f23} < 0.45; \quad 0.4 < V_f < 0.7 \tag{18}$$

Equation (18) presents the range of material constants for composites with transversely isotropic fibers. For composites using completely isotropic fibers, the ranges were $20 < E_f/E_m < 120$ and $0.2 < \nu_f < 0.35$. Design points were generated based on the variables listed in Eq. (18). The selection of the design of experiments was performed with a criterion for minimizing the minimum distance between any two design points in the design space. One hundred designs for composites with transversely isotropic fibers and 40 for composites with isotropic fibers were generated. In an effort to make the numerical ranges across all the variables more uniform, the logarithms of some of the design variables were used. The five variables used in constructing the response surface are as follows:

$$\log_{10}\left(\frac{E_{f1}}{E_m}\right); \qquad \log_{10}\left(\frac{E_{f2}}{E_m}\right); \qquad \frac{\nu_{f12}}{\nu_m}; \qquad \frac{\nu_{f23}}{\nu_m}; \qquad V_f \tag{19}$$

The design points generated using the variables in Eq. (18) were propagated to the set of variables in Eq. (19). The matrix properties were taken as $E_m = 1$ and $\nu_m = 0.35$.

For each simulation, a set of parameters $T_{22}$ and $T_{32}$ was obtained (i.e., 140 sets of parameters were recorded). Thus, independent response surfaces were constructed for the prediction of $T_{22}$ and $T_{32}$. An initial predictive capability test involving various types (full and reduced) and degrees of polynomial response surfaces was carried out, for six practical composite design systems (material details provided in Table 2), to check the average error in prediction of each fit. With 140 data points available, response surfaces were constructed and tested for polynomials of degrees one through four [15].

It is important to note that Table 3 only displays the most accurate response surfaces that were selected for the prediction of $T_{22}$ and $T_{32}$. The reader may refer to [15] for the comparison of other response surfaces that were tested. We may now proceed with in-depth result analysis using the selected response surfaces. The reader may use their own variable ranges to construct response surfaces or may use the fits from Table 3, the coefficients of which have been provided in [15]. The average error in prediction of $T_{22}$ and $T_{32}$ was computed over the six composite models analyzed using finite element analysis with a volume fiber fraction of 0.6 and material properties listed in Table 2. The range of $T_{22}$ varied from 0.025 to 1.12. To increase the absolute minimum value of the response (it was observed that the predictive capability of the fit increased by doing so), the variables are fit against $\log_{10}(T_{22})$, which has a range of $-1.60$ to 0.05. The range of $T_{32}$ varies from $-0.022$ to 0.071. Again to increase the predictive capability of the fit the variables are fit against $10^{T_{32}}$, which has a range of 0.950 to 1.18. Note that a reduced fit was used to predict $T_{32}$. A reduced fit removes the coefficients (using $t$-statistics), which do not contribute much to the response surface predictive capability.

**Table 2 Material properties [13,17,18] in GPa units for validation of response surfaces**

| Material | $E_{f1}$ | $E_{f2}$ | $\nu_{f12}$ | $\nu_{f23}$ | $G_{f12}$ |
|---|---|---|---|---|---|
| | | *Fiber properties* | | | |
| T-300 | 221 | 13.8 | 0.200 | 0.430 | 8.96 |
| Graphite | 263 | 19.0 | 0.200 | 0.350 | 27.6 |
| Kevlar | 152 | 4.14 | 0.350 | 0.361 | 2.90 |
| S-glass | 85.5 | 85.5 | 0.200 | 0.200 | 35.6 |
| E-glass | 73.1 | 73.1 | 0.220 | 0.220 | 30.1 |
| Boron | 400 | 400 | 0.200 | 0.200 | 167 |
| | | *Matrix properties* | | | |
| Epoxy | 3.50 | 3.50 | 0.350 | 0.350 | 1.29 |

**Table 3 Accuracy and predictive capability characteristics of response surfaces**

| Type | Degree of polynomial | N-PRESS RMSE,[a] % | NRMSE,[a] % | Adjusted goodness of fit ($R_a^2$)[a] | Average error in prediction % | Number of coefficients |
|---|---|---|---|---|---|---|
| Full ($T_{22}$) | 3 | 0.34 | 0.11 | 1.00 | 0.621 | 56 |
| Reduced ($T_{32}$) | 4 | 7.87 | 0.12 | 0.999 | 6.09 | 89 |

[a]Refer to appendices for details.

## IV. Result Analysis

### A. Evaluation of the Two-Parameter Model

We compare the results from the two-parameter model (TPM) with that from direct FEA for two composites, one using a transversely isotropic fiber (graphite) and the second using an isotropic fiber (E-glass).

Figure 4 displays the accuracy of two different methods (the two-parameter model using polynomial response surfaces and the rule of mixtures) and their comparison, with respect to the results obtained using FEA, for predicting the material properties of the graphite epoxy composite.

Figure 5 displays the accuracy of the two-parameter-based response surface and rule of mixtures as well as their comparison with respect to the results obtained using FEA, for predicting the material properties of the E-glass epoxy composite.

As mentioned previously, the widely used Halpin–Tsai model (used to predict the transverse elastic and shear modulus) is valid for composite models with square unit cells only [14]. Hence, a comparison with the Halpin–Tsai model would not have been a reasonable assessment.

### B. Comparison to Prediction using Response Surface for the Elastic Constants

One of the questions raised by the analysis of the response surfaces (used to predict $T_{22}$ and $T_{32}$) was how good these approximations are compared to a response surface where one might fit directly the elastic constants to the composite designs. As portrayed by error estimates in Table 4, there is not significant amount of difference between the two approaches.

## V. Predicting the Longitudinal Shear Modulus

As stated previously, the two-parameter model does not predict the transverse shear modulus $G_{12}$. However, to maintain completeness, a surrogate for $G_{12}$ is also presented here. The method to predict $G_{12}$ using a plane model of the unit cell as described in [5] was used. The procedures for hexagonal unit cell are further described in detail in [15]. A unit shear-strain analysis was performed for each of the 100 transversely isotropic designs generated for the two-parameter model.

The design variables were $\log_{10}(G_{f12}/G_m)$ and $V_f$. Various response surfaces were constructed to a find the most accurate fit between the variables and the longitudinal shear modulus of the composite, $G_{12}$. The high number of data points and low number of variables allowed for the construction of full response surfaces with order of polynomials as high as four. The most accurate amongst all the response surfaces, the fourth-degree fit, was found to give an average prediction error of less than 0.1% (see Table 5). The coefficients of the fourth-degree fit have been provided in [15]. However, the second-degree response surface given next appears to be a reasonable approximation for practical applications:

$$\frac{G_{12}}{G_m} = 2 - 0.65\log_{10}\left(\frac{G_{f12}}{G_m}\right) - 5.6V_f - 0.15\left(\log_{10}\left(\frac{G_{f12}}{G_m}\right)\right)^2 + 2.7V_f\log_{10}\left(\frac{G_{f12}}{G_m}\right) + 4.4V_f^2 \tag{20}$$

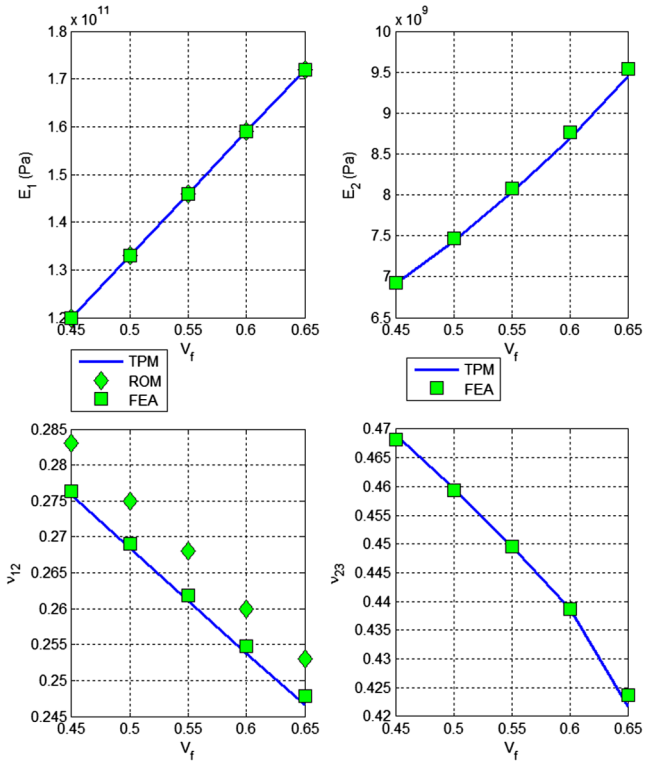


**Fig. 4 Comparison of elastic constants of graphite/epoxy composite obtained using the TPM and response surface for FEA results. Rule of mixtures results are given for $E_1$ and $\nu_{12}$ for comparison.**

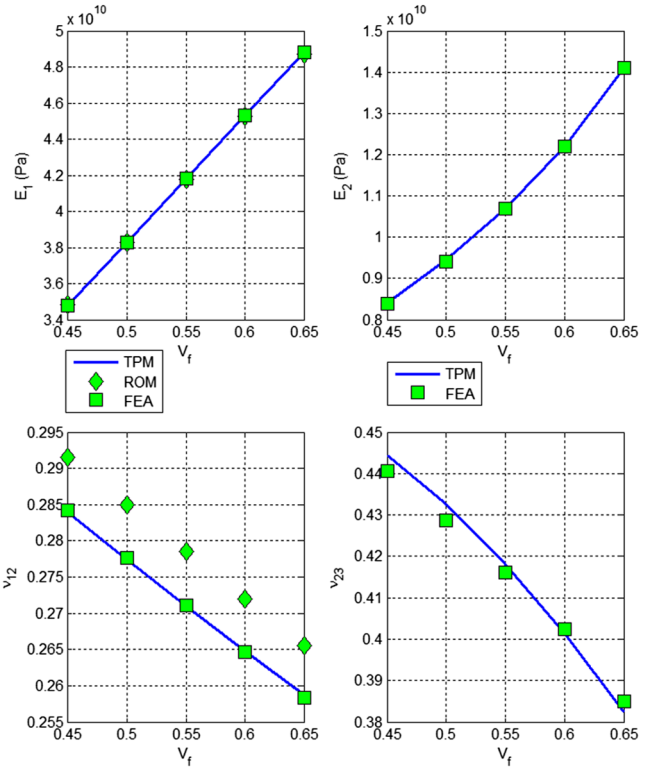


**Fig. 5 Comparison of elastic constants of E-glass/epoxy composite obtained using the TPM and response surface for FEA results. Rule of mixtures results are given for $E_1$ and $\nu_{12}$ for comparison.**

**Table 4 Error comparison between response surfaces for the two parameters and elastic constants**

| $V_f$ | Constants (predicted by) | Percent error in $E_1$ | Percent error in $\nu_{12}$ | Percent error in $E_2$ | Percent error in $\nu_{23}$ |
|---|---|---|---|---|---|
| 0.45 | Response surface for $T_{22}$ and $T_{32}$. | 0.001 | 0.096 | 0.382 | 0.617 |
| 0.45 | Response surface for $E_1$, $E_2$,$\nu_{12}$, and $\nu_{23}$ | 0.033 | 0.048 | 0.593 | 0.139 |
| 0.5 | Response surface for $T_{22}$ and $T_{32}$. | 0.001 | 0.106 | 0.315 | 0.557 |
| 0.5 | Response surface for $E_1$, $E_2$,$\nu_{12}$, and $\nu_{23}$ | 0.010 | 0.023 | 0.405 | 0.162 |
| 0.55 | Response surface for $T_{22}$ and $T_{32}$. | 0.000 | 0.077 | 0.216 | 0.200 |
| 0.55 | Response surface for $E_1$, $E_2$,$\nu_{12}$, and $\nu_{23}$ | 0.012 | 0.030 | 0.440 | 0.194 |
| 0.6 | Response surface for $T_{22}$ and $T_{32}$. | 0.001 | 0.144 | 0.335 | 0.593 |
| 0.6 | Response surface for $E_1$, $E_2$,$\nu_{12}$, and $\nu_{23}$ | 0.018 | 0.038 | 0.620 | 0.240 |
| 0.65 | Response surface for $T_{22}$ and $T_{32}$. | 0.002 | 0.196 | 0.389 | 0.892 |
| 0.65 | response surface for $E_1$, $E_2$,$\nu_{12}$, and $\nu_{23}$ | 0.026 | 0.047 | 0.892 | 0.361 |

**Table 5 Accuracy and predictive capability characteristics of response surfaces for prediction of $G_{12}$**

| Type | N-PRESS RMSE, % | NRMSE, % | Adjusted goodness of fit ($R_a^2$) | Average error in prediction, % | Number of coefficients |
|---|---|---|---|---|---|
| First degree | 6.14 | 5.80 | 0.917 | 4.10 | 3 |
| Second degree | 1.37 | 1.21 | 0.996 | 1.48 | 6 |
| Third degree | 0.588 | 0.368 | 0.999 | 0.385 | 10 |
| Fourth degree | 0.132 | 0.066 | 1.00 | 0.098 | 15 |

**Table 6 Error comparison in prediction of $G_{12}$**

| Fiber | $G_{12}$ computed using finite elements, GPa | Percent error in prediction of $G_{12}$ using Eq. (A3) | Percent error in prediction of $G_{12}$ using third-degree response surface | Percent error using Halpin–Tsai equations with $\zeta = 1$ |
|---|---|---|---|---|
| Graphite | 4.41 | 0.78 | 0.16 | 0.32 |
| T-300 | 3.40 | 1.15 | 0.75 | 0.11 |
| E-glass | 4.47 | 2.1 | 0.24 | 0.32 |
| S-glass | 4.56 | 1.19 | 0.31 | 0.34 |



Although the results here are for a hexagonal unit cell, it is found that the Halpin–Tsai equation for $G_{12}$ for a circular fiber in a square unit cell available in the literature (e.g., [13]) is as accurate as the third-degree response surface as shown in Table 6. A value of $\zeta = 1$ was used in the Halpin–Tsai equations.

## VI. Conclusions

A new micromechanics method called the two-parameter model was derived for the prediction of $E_1, E_2, \nu_{12}$, and $\nu_{23}$ of a transversely isotropic fiber composite. Only one plane micromechanics analysis of the unit cell is required to determine the two parameters. Surrogate modeling of the two parameters for composites with hexagonal unit cell using polynomial response surfaces was carried out for the accurate prediction of the two parameters as a function of several variables that describe the microstructure of the composite. The response surfaces were constructed based on the results obtained from 140 individual simulations of composite designs generated using Latin hypercube sampling. The results indicate that the two-parameter model results are as accurate as that from a complete finite-element analysis of the unit cell. A separate response surface was developed for the prediction of the longitudinal shear modulus $G_{12}$. The empirical results for elastic constants will be useful in the design, optimization, and sensitivity studies of unidirectional fiber composites.

## Appendix A: Error Measures for Surrogate Modeling

A response surface methodology portrays the relationship between several explanatory (independent) variables and one or more response (dependent) variables. In its most generic form, a response function $y$ (that needs to be approximated) can be denoted as a combination of $\hat{y}$ (approximated function of a design variable vector $x$ and a vector of unknown parameters, $\beta$) and $e$, the vector of errors associated with the curve fit:

$$y_i = \hat{y}(x_i, \beta) + e_i \tag{A1}$$

One has the data obtained from $n_y$ experiments at $n_y$ design points. Each design point is denoted by $x_i$. Our main objective is to find the set of parameters $\beta$, that will best fit the experimental data. The process of finding the vector $\beta$ that best fits the experimental data is called regression, and $\hat{y}$ is called a response surface.

### A1 Normalized Root-Mean-Square Error

Normalized rms error (N-RMSE) is one of the most commonly used measures of the error observed while approximating a response is the rms error and is given by

$$e_{\text{rms}} = \sqrt{\frac{1}{n_y}\sum_{i=1}^{n_y}(y_i - \hat{y}(x_i, \beta))^2} \tag{A2}$$

N-RMSE is a much more comparable measure of the rms error because it can be measured in percentage. In the presented study, N-RMSE is calculated by dividing the rms error by the range of observed values. The expression for normalized rms error is thus given by

$$e_{N\text{-rms}} = \frac{\sqrt{\frac{1}{n_y}\sum_{i=1}^{n_y}(y_i - \hat{y}(x_i, \beta))^2}}{\max(y) - \min(y)} \tag{A3}$$

Cross validation is an important aspect of surrogate modeling. It is particularly attractive because it does not require any extra sets of experiments to be performed. A cross-validation error is the error at a data point when the surrogate is fitted to a subset of the $p$ data points that does not include this point. This can only be done provided the number of points used for the fit is substantially larger than the number of coefficients. When the surrogate is fitted to all the other $n_y - 1$ points, the process has to be repeated $n_y$ times (leave-one-out strategy) to obtain the vector of cross validation errors, $e_{\text{cv}}$ [16]. Because we are

using the sum of the squares of the prediction errors as a measure of the predictive accuracy of the response surface, the error is termed as prediction error sum of squares (PRESS) rms error:

$$\text{PRESS}_{\text{rms}} = \sqrt{\frac{1}{n_y} e_{\text{cv}}^T e_{\text{cv}}} \tag{A4}$$

We will make use of the normalized PRESS rms error (N-PRESS RMSE, normalized in a manner similar to that of NRMSE).

## A2 Adjusted Goodness of Fit

Another popular way for evaluating the accuracy of the fit is by calculating the variation of the data throughout the response surface. The variation of the data from its average $\bar{y}$ is given by $SS_y$. The variation of the response surface from that same average is given by $SS_R$. Thus,

$$SS_y = \sum_{i=1}^{n_y} (y_i - \bar{y})^2, \qquad SS_r = \sum_{i=1}^{n_y} (\hat{y}_i - \bar{y})^2 \tag{A5}$$

The ratio of $SS_R$ to $S_y$, denoted by $R^2$, measures the fraction of the variation in data as captured by the response surface. Increasing the number of coefficients increases the value of $R^2$. This by no means conveys the statement that the prediction capabilities of the response surface have improved. For $n_\beta$ coefficients, the adjusted form of $R^2$ is given by

$$R_a^2 = 1 - (1 - R^2)\left(\frac{n_y - 1}{n_y - n_\beta}\right) \tag{A6}$$

Thus, the adjusted value of $R^2$ is a better measure of goodness of fit. It is important to note that, if this value decreases upon increasing the number of coefficients, it is a sign that we might be fitting the data better but losing out on the predictive capabilities of the response surface.

## References


[1] Christensen, R. M., *Mechanics of Composite Materials*, 1st ed., Dover, Mineola, NY, 2005, p. 58.

[2] Eshelby, J. D., "The Determination of the Elastic Field of an Ellipsoidal Inclusion, and Related Problems," *Proceedings of the Royal Society of London, Series A: Mathematical and Physical Sciences*, Vol. 241, No. 1226, Aug. 1957, pp. 376–396. doi:10.1098/rspa.1957.0133

[3] Halpin, J. C., "Effects of Environmental Factors on Composite Materials," AFML TR-67-423, Wright–Patterson AFB, OH, 1969.

[4] Sun, C. T., and Chen, J. L., "A Micromechanical Model for Plastic Behavior of Fibrous Composites," *Composites Science and Technology*, Vol. 40, No. 2, 1991, pp. 115–129. doi:10.1016/0266-3538(91)90092-4

[5] Zhu, H., Sankar, B. V., and Marrey, R. V., "Evaluation of Failure Criteria for Fiber Composites Using Finite Element Micromechanics," *Journal of Composite Materials*, Vol. 32, No. 8, 1998, pp. 766–782. doi:10.1177/002199839803200804

[6] Jadhav, V. R., and Sridharan, S., "Prediction of Nonlinear Behavior of Composites via Micromechanics Using Matrix Bulk Properties," *AIAA Journal*, Vol. 41, No. 11, 2003, pp. 2229–2238. doi:10.2514/2.6815

[7] Dang, T. D., and Sankar, B. V., "Meshless Local Petrov–Galerkin Formulation for Problems in Composite Micromechanics," *AIAA Journal*, Vol. 45, No. 4, 2007, pp. 912–921. doi:10.2514/1.23434

[8] Rakow, J. F., and Waas, A. M., "On the Effective Isotropic Moduli of Random Fibrous Composites, Platelet Composites, and Foamed Solids," *Mechanics of Advanced Materials and Structures*, Vol. 11, No. 2, 2014, pp. 151–173. doi:10.1080/15376490490277286

[9] Chou, T. W., and Ishikawa, T., "One-Dimensional Micromechanical Analysis of Woven Fabric Composites," *AIAA Journal*, Vol. 21, No. 12, 1983, pp. 1714–1721. doi:10.2514/3.8314

[10] Bednarcyk, B. A., and Arnold, S. M., "Micromechanics-Based Modeling of Woven Polymer Matrix Composites," *AIAA Journal*, Vol. 41, No. 9, 2003, pp. 1788–1796. doi:10.2514/2.7297

[11] Tabiei, A., Jiang, Y., and Yi, W., "Novel Micromechanics-Based Woven-Fabric Composite Constitutive Model with Material Nonlinear Behavior," *AIAA Journal*, Vol. 38, No. 8, 2000, pp. 1437–1443. doi:10.2514/2.1120

[12] Weigand, J. P., and TerMaath, S. C., "Sensitivity Analysis of Out-of-Plane Composite Lamina Properties Relative to Configuration and Constitutive Properties," *55th AIAA/ASME/ASCE/AHS/SC Structures, Structural Dynamics, and Materials Conference*, AIAA Paper 2014-1373, 2014.

[13] Gibson, R. F., *Principles of Composite Material Mechanics*, 3rd ed., CRC Press, Boca Raton, FL, 2012, pp. 105–117.

[14] Banarjee, S., and Sankar, B. V., "Mechanical Properties of Hybrid Composites Using Finite Element Method Based Micromechanics," *Composites Part B: Engineering*, Vol. 58, March 2014, pp. 318–327. doi:10.1016/j.compositesb.2013.10.065

[15] Sharma, A., "Micromechanics of Composites Using a Two-Parameter Model and Response Surface Prediction of Its Properties," M.S. Thesis, Dept. of Mechanical and Aerospace Engineering, Univ. of Florida, Gainesville, FL, 2013.

[16] Viana, F. A. C., "Multipe Surrogate for Prediction and Optimization," Ph.D. Dissertation, Dept. of Mechanical and Aerospace Engineering, Univ. of Florida, Gainesville, FL, 2013.

[17] Stamblewski, C., Sankar, B. V., and Zenkert, D., "Analysis of Three-Dimensional Quadratic Failure Criteria for Thick Composites Using the Direct Micromechanics Method," *Journal of Composite Materials*, Vol. 42, No. 7, 2008, pp. 635–654. doi:10.1177/0021998307088609

[18] Choi, S., and Sankar, B. V., "Micromechanical Analysis of Composite Laminates at Cryogenic Temperatures," *Journal of Composite Materials*, Vol. 40, No. 12, 2005, pp. 1077–1091. doi:10.1177/0021998305057365

[19] Box, G. E. P., and Wilson, K. B., "On the Experimental Attainment of Optimum Conditions," *Journal of the Royal Statistical Society, Series B*, Vol. 13, No. 1, 1950, pp. 1–45. doi:10.1007/978-1-4612-4380-9_23

[20] Queipo, N. V., Haftka, R. T., Shyy, W., Goel, T., Vaidyanathan, R., and Tucker, K. P., "Surrogate Based Analysis and Optimization," *Progress in Aerospace Sciences*, Vol. 41, No. 1, 2005, pp. 1–28. doi:10.1016/j.paerosci.2005.02.001

[21] Myers, R. H., and Montgomery, D. C., *Response Surface Methodology: Process and Product Optimization Using Design Experiment*, Wiley, New York, 1995, pp. 1–12.


R. Kapania
*Associate Editor*